

# Niemann-Pick C1-Like 1 deletion in mice prevents high-fat diet-induced fatty liver by reducing lipogenesis<sup>§</sup>

Lin Jia, Yinyan Ma, Shunxing Rong, Jenna L. Better, Ping Xie, Soonkyu Chung, Nanping Wang, Weiqing Tang, and Liqing Yu<sup>1</sup>

Department of Pathology Section on Lipid Sciences, Wake Forest University School of Medicine, Medical Center Boulevard, Winston-Salem, NC 27157-1040

**Abstract** Niemann-Pick C1-Like 1 (NPC1L1) mediates intestinal absorption of dietary and biliary cholesterol. Ezetimibe, by inhibiting NPC1L1 function, is widely used to treat hypercholesterolemia in humans. Interestingly, ezetimibe treatment appears to attenuate hepatic steatosis in rodents and humans without a defined mechanism. Overconsumption of a high-fat diet (HFD) represents a major cause of metabolic disorders including fatty liver. To determine whether and how NPC1L1 deficiency prevents HFD-induced hepatic steatosis, in this study, we fed NPC1L1 knockout (L1-KO) mice and their wild-type (WT) controls an HFD, and found that 24 weeks of HFD feeding causes no fatty liver in L1-KO mice. Hepatic fatty acid synthesis and levels of mRNAs for lipogenic genes are substantially reduced but hepatic lipoprotein-triglyceride production, fatty acid oxidation, and triglyceride hydrolysis remain unaltered in L1-KO versus WT mice. Strikingly, L1-KO mice are completely protected against HFD-induced hyperinsulinemia under both fed and fasted states and during glucose challenge. Despite similar glucose tolerance, L1-KO relative WT mice are more insulin sensitive and in the overnight-fasted state display significantly lower plasma glucose concentrations. **In conclusion, NPC1L1 deficiency in mice prevents HFD-induced fatty liver by reducing hepatic lipogenesis, at least in part, through attenuating HFD-induced insulin resistance, a state known to drive hepatic lipogenesis through elevated circulating insulin levels.**—Jia, L., Y. Ma, S. Rong, J. L. Better, P. Xie, S. Chung, N. Wang, W. Tang, and L. Yu. **Niemann-Pick C1-Like 1 deletion in mice prevents high-fat diet-induced fatty liver by reducing lipogenesis.** *J. Lipid Res.* 2010. 51: 3135–3144.

**Supplementary key words** ezetimibe • nonalcoholic fatty liver disease • intestinal cholesterol absorption • insulin resistance • obesity

*This work was supported in part by a Scientist Development Grant #0635261N from the American Heart Association (to L.Y.) and by Award Number R01DK085176 from the National Institute of Diabetes and Digestive and Kidney Diseases (to L.Y.). The content is solely the responsibility of the authors and does not necessarily represent the official views of the National Institute of Diabetes and Digestive and Kidney Diseases or the National Institutes of Health or other granting agencies. J.L.B. is supported by a Ruth L. Kirschstein National Research Service Award (NRSA) (#1F32DK084582-01) provided by the National Institute of Diabetes and Digestive and Kidney Diseases.*

*Manuscript received 24 February 2010 and in revised form 10 August 2010.*

*Published, JLR Papers in Press, July 24, 2010  
DOI 10.1194/jlr.M006353*

Copyright © 2010 by the American Society for Biochemistry and Molecular Biology, Inc.

This article is available online at <http://www.jlr.org>

Niemann-Pick C1-Like 1 (NPC1L1) is a polytopic transmembrane protein essential for intestinal absorption of both biliary and dietary cholesterol (1, 2). The tissue distribution of NPC1L1 expression differs among species. In humans, NPC1L1 is abundantly expressed in both small intestine and liver (2–4). In rodents, NPC1L1 is almost exclusively expressed in the small intestine where it resides at the apical membrane of absorptive enterocytes (2). NPC1L1 knockout (L1-KO) mice are resistant to high-cholesterol diet-induced hypercholesterolemia due to a substantial reduction in intestinal cholesterol absorption (2, 5, 6).

NPC1L1 is the target of ezetimibe (7, 8), a potent cholesterol absorption inhibitor that is widely used to lower blood low density lipoprotein (LDL)-cholesterol in humans (9). Unexpectedly, ezetimibe treatment or NPC1L1 deficiency was recently shown to improve many metabolic disorders besides hypercholesterolemia in rodents and in obese humans (10, 11). For instance, ezetimibe treatment lessened hepatic steatosis and improved insulin sensitivity in leptin receptor-deficient Zucker obese rats (12, 13). Ezetimibe also reduced hepatic steatosis in mice on the methionine choline-deficient diet (14) or diets containing high amounts of cholesterol (15). In a study focusing on obesity and diabetes, ezetimibe treatment or NPC1L1 deficiency was shown to attenuate weight gain and insulin resistance in mice on a high-fat diet (HFD), though it remains to be determined whether this intervention influences the development of hepatic steatosis (16). In another study focusing on the role of NPC1L1 in protein

Abbreviations: BW, body weight; ChREBP, carbohydrate responsive element-binding protein; ER, endoplasmic reticulum; H and E, hematoxylin and eosin; HFD, high-fat diet; HLM, hypotonic lysis medium; L1-KO, NPC1L1 knockout; LXR, liver X receptor; NAFLD, non-alcoholic fatty liver disease; NPC1L1, Niemann-Pick C1-Like 1; ROS, reactive oxygen species; qPCR, quantitative real-time PCR; SREBP, sterol regulatory element-binding protein; TBARS, thiobarbituric acid reactive substrate; WT, wild-type.

<sup>1</sup>To whom correspondence should be addressed.

e-mail: [lyu@wfubmc.edu](mailto:lyu@wfubmc.edu)

<sup>§</sup>The online version of this article (available at <http://www.jlr.org>) contains supplementary data in the form of two tables.

trafficking and diet-induced hypercholesterolemia, L1-KO mice were observed to be resistant to hepatic steatosis induced by the Paigen diet, a lithogenic diet that contains high amounts of bile acid and cholesterol (3). Additionally, ezetimibe treatment significantly decreased hepatic triglyceride content in obese humans on a weight loss diet (10). Despite these interesting observations, mechanisms by which NPC1L1 deficiency or ezetimibe treatment alleviates hepatic steatosis, insulin resistance, and obesity remain largely unexplored.

Hepatic steatosis, steatohepatitis, fibrosis, and cirrhosis are collectively known as nonalcoholic fatty liver disease (NAFLD) (17). In the general population, the estimated prevalence of NAFLD could be as high as 24% (18). Hepatic steatosis may occur in 17–33% of Americans (19), representing a burgeoning health problem worldwide. Fat overconsumption plays an important role in the etiology of hepatic steatosis. Effects of NPC1L1 deficiency on HFD-induced hepatic steatosis have not been examined. Earlier studies were performed with animals that were either deficient in leptin pathway (12, 13) or challenged with a non-physiological diet (3, 14) or a diet containing high amounts of cholesterol (15).

Different diets cause hepatic steatosis likely through distinct mechanisms. For animals on a high-cholesterol diet, it is conceivable that NPC1L1 deficiency or ezetimibe treatment may reduce hepatic steatosis by attenuating cholesterol-dependent liver X receptor (LXR) activation (20) and LXR activation-induced lipogenesis (21) through limiting intestinal cholesterol absorption. Consistent with this, we found that L1-KO relative to wild-type (WT) mice accumulate less triglyceride in liver after treatment with T0901317 (22), a synthetic LXR agonist that promotes hepatic lipogenesis (21). During HFD feeding, animals develop insulin resistance, a pathological state that is associated with elevated circulating insulin levels. In this state, the liver is selectively resistant to insulin-induced suppression of gluconeogenesis, but stays sensitive to insulin-stimulated activation of sterol regulatory element-binding protein (SREBP)-1c (23), a membrane-bound transcription factor whose activation promotes lipogenesis (24), thereby developing steatosis (25). Hepatic steatosis itself may in turn dampen insulin signaling and therefore aggravate hepatic and systemic insulin resistance (26). This vicious cycle represents an important mechanism underlying HFD-induced insulin resistance and hepatic steatosis. We hypothesized that NPC1L1 deficiency may prevent HFD-induced hepatic steatosis mainly by stopping this vicious cycle. Consistent with this hypothesis, in this study, we showed that 24 weeks of HFD feeding does not cause hepatic steatosis in L1-KO mice and the plasma insulin level is reduced by ~85% in these animals relative to WT mice, which is associated with substantially reduced hepatic fatty acid synthesis and levels of mRNAs for all the lipogenic genes examined. Thus, the HFD-driven insulin resistance-hepatic steatosis vicious cycle was completely blocked in NPC1L1-deficient mice. Our findings may promote clinical studies of ezetimibe effects on hepatic steatosis and the associated metabolic disorders in humans.

## Animals and diets

L1-KO mice of pure C57BL/6 background were reported previously (3). All mice were housed in a specific pathogen-free animal facility in plastic cages at 22°C with a daylight cycle from 6AM to 6PM. The mice were provided with water and standard chow diet (Prolab RMH 3000) ad libitum unless stated otherwise. All animal procedures were approved by the Institutional Animal Care and Use Committee at Wake Forest University Health Sciences. Male L1-KO mice and their WT controls were fed an HFD (TD.93075; Harlan Teklad, Madison, WI) for 24 weeks starting at 6 weeks of age. The HFD derives 54.8% calories from fat, 21.2% calories from protein, and 24% calories from carbohydrates. It contains only a trace amount of cholesterol (~0.007%). The fatty acid composition in the fat of this diet is 28% saturated-, 30% monounsaturated-(trans), 28% monounsaturated-(cis), and 14% polyunsaturated-(cis) fatty acids (27).

## Fecal neutral sterol excretion and intestinal cholesterol absorption

After 18 weeks on an HFD, mice were used for the determination of fecal neutral sterol excretion and intestinal cholesterol absorption as we have described previously (28).

## Intestinal fat absorption

After 13 weeks on an HFD, mice were individually housed and fed for 7 days a test diet with a composition similar to the HFD except 5% of fat in the test diet was replaced by the nonabsorbable marker, sucrose poly-behenate (29). The test diet was prepared by our diet core in the primate center of Wake Forest University Health Sciences. In the last 3 days of test diet feeding, fecal samples were collected. The fatty acid content and composition in both the diet and feces were determined by gas chromatography and the fractional absorption of total and individual fatty acids was calculated as described previously (29).

## Blood biochemistries

Plasma insulin and adiponectin were measured by Ultra Sensitive Mouse Insulin ELISA Kit (Crystal Chem, Inc.) and Quantikine Mouse Adiponectin/Acrp30 (R & D Systems), respectively. Fed and fasted plasma glucose levels were measured by Glucose Assay Kit (Cayman Chemical Co.). Plasma  $\beta$ -hydroxybutyrate (LiquiColor, Stanbio) and nonesterified fatty acids [HR Series NEFA-HR (2), Wako] were measured following the manufacturer's instructions. Plasma concentrations of total cholesterol, free cholesterol, and triglyceride were analyzed using the Cholesterol/HP (Roche), the Free Cholesterol C (Wako), and Triglycerides/GB (Roche) enzymatic assay kits, respectively.

## Liver lipids

After a 4 h fast during the daylight cycle, mice were euthanized after bleeding and livers removed and snap-frozen in liquid nitrogen for liver lipid analysis as we have described previously (4).

## Liver histopathology

Livers were fixed in 10% buffered formalin and processed for hematoxylin and eosin (H and E) staining in the clinical laboratory of our department.

## De novo cholesterol and fatty acid synthesis in liver

These measurements were performed as described previously by Mulvihill, et al. (30). After 6 weeks of HFD feeding, mice were fasted for 4 h followed by intraperitoneal injection of 10  $\mu$ Ci of

[1-<sup>14</sup>C]acetic acid (PerkinElmer, Boston, MA). One hour later, mice were euthanized. Liver tissues (~250 mg) were collected, saponified in 2.2 ml of a mixture of 50% potassium hydroxide in water and 95% ethanol (1:10), and then extracted by 3 ml of hexane. The sterol-containing hexane extract was dried down by nitrogen gas and then solubilized in scintillation cocktail for scintillation counting for the determination of de novo hepatic cholesterol synthesis. The remaining aqueous phase was acidified with 0.8 ml of glacial acetic acid (pH 6), extracted by 3 ml of hexane, and processed for scintillation counting for the determination of de novo hepatic fatty acid synthesis.

### Hepatic fatty acid oxidation

Fatty acid oxidation activity was measured as previously described (31). After 6 weeks of HFD feeding, mice were fasted for 4 h. Fresh liver tissue (~200 mg) was homogenized in four volumes of 0.25 M sucrose containing 1 mM EDTA. About 5 mg of tissue homogenate was incubated for 30 min at 25°C in a buffer containing 150 mM KCl, 10 mM HEPES (pH 7.2), 0.1 mM EDTA, 1 mM potassium phosphate buffer (pH 7.2), 5 mM malonate, 10 mM MgCl<sub>2</sub>, 1 mM carnitine, 0.15% fatty acid free-BSA, 5 mM ATP, and 50 μM palmitic acid containing 1 μCi of [9,10(n)-<sup>3</sup>H] palmitic acid (PerkinElmer). Reactions were stopped with the addition of 200 μl 0.6 N perchloric acid. Unreacted fatty acids were removed by hexane extraction. Radioactive degradation products in the aqueous phase were counted and the data were presented as DPM/min/mg liver protein.

### Liver triglyceride production

Hepatic triglyceride production was measured as described previously (32). After a 4 h fast, mice were anesthetized and injected with Tyloxapol (Triton WR-1339) (Sigma) at 500 mg/kg body weight (BW) via the retro-orbital vein to block lipolysis. Each mouse received ~100 μl of saline solution containing 15 g/dl Tyloxapol. Blood samples were collected at 0, 30, 60, 90, 120, and 180 min after injection. Plasma triglyceride concentrations were measured by the enzymatic assay described above. Linear regression line was drawn against plasma triglyceride concentrations of individual animals versus their corresponding time points using GraphPad Prism 5. The triglyceride secretion rate was derived from the slope of the line.

### Liver triglyceride hydrolase activity

Liver triglyceride hydrolase activity was measured in the cytosolic extracts of livers from LI-KO and WT mice fed an HFD for 24 weeks as described previously using lipid droplets isolated from HepG2 cells as substrates (33, 34). For radioactive labeling of lipid droplets, HepG2 cells were treated with 2.5 μCi [<sup>3</sup>H-9,10] oleic acid/ml + 0.8 mM cold oleic acid complexed to BSA for 16 h. Cells were then washed with ice-cold PBS and centrifuged (1000 g at 4°C for 10 min). The supernatant was removed and the cells were resuspended in ice-cold hypotonic lysis medium (HLM) (20 mM Tris-HCl, pH 7.4, 1 mM EDTA, 10 mM sodium fluoride, and protease inhibitor cocktail). To isolate lipid droplets, resuspended cells were transferred to a Potter-Elvehjem tissue homogenizer and gently homogenized on ice. After centrifugation, the supernatant and floating fat layer were collected and adjusted to a final concentration of 20% sucrose in HLM. This was layered into a 13.2 ml ultracentrifuge tube and gently overlaid with 5 ml ice-cold HLM containing 5% sucrose. The remainder of the tube was filled with HLM and centrifuged at 28,000 g at 4°C for 30 min using an SW40 rotor. The floating white lipid droplet layer was collected and triglyceride (TG) contents were determined enzymatically. For the determination of hepatic triglyceride hydrolase activity, the cytosolic extracts were prepared by homogenizing liver samples in buffer A (0.25 M su-

crose, 1 mM EDTA, 1 mM DTT, and protease inhibitor cocktail). Homogenate was centrifuged at 20,000 g for 30 min at 4°C. The infranatant was removed and ultracentrifuged at 100,000 g for 1 h at 4°C. One hundred micrograms of the triglyceride-free infranatant was incubated with 25 nmol [<sup>3</sup>H-9,10]oleate labeled lipid droplet substrate and 5% BSA in a total volume of 200 μl for 1 h at 37°C. The reaction was stopped by adding 3.25 ml of methanol:chloroform:heptane (10:9:7) and 1 ml of 0.1 M potassium carbonate, and 0.1 M boric acid (pH 10.5). After centrifugation, the radioactivity in 1 ml of the upper phase was determined by scintillation counting.

### Glucose and insulin tolerance tests

For glucose tolerance tests, mice were fasted for 10 h. After measuring the baseline blood glucose level via a tail nick using a Glucometer (Bayer Contour), a 20% glucose solution was injected intraperitoneally at 1.5 mg/g BW. Blood glucose levels were then measured at 15, 30, 60, and 120 min after glucose injection. For insulin tolerance tests, mice were fasted for 6 h. After measuring the baseline blood glucose level, mice were injected intraperitoneally with recombinant human insulin (Novo Nordisk, Inc.) at 1.2 mU/g BW, and their blood glucose concentrations were determined at 15, 30, 60, and 120 min post insulin administration.

### Glucose-stimulated insulin secretion

Glucose-stimulated insulin secretion was performed as described (35). Seven-week-old chow fed WT mice or 6-week-old WT and LI-KO mice on an HFD for 5 weeks were fasted for 10 h and a bolus of 20% glucose was injected into the intraperitoneal cavity at 1.5 mg/g BW. Blood samples were collected at 0, 15, and 30 min from tails for plasma insulin determination using an ELISA kit (Crystal Chem, Inc.).

### qPCR

The quantitative real-time PCR (qPCR) was performed as described previously (36). All primers used for qPCR are available upon request.

### Hepatic oxidative stress

Hepatic levels of the lipid peroxidation product malondialdehyde were measured as thiobarbituric acid reactive substrates (TBARS) using the TBARS Assay Kit (Cayman Chemical Co.). Hepatic redox environment was determined by measuring glutathione (GSH)/oxidized glutathione (GSSG) ratio using Glutathione Assay Kit (Cayman Chemical Co.).

### Statistical analysis

Data are expressed as mean ± SEM. The difference between the mean values of LI-KO and WT groups was tested for statistical significance by two-tailed Student's *t*-tests. A value of *P* < 0.05 was accepted as statistically significant.

## RESULTS

### NPC1L1 deficiency promotes loss of endogenous cholesterol in mice on an HFD

Currently, there are no studies of the effects of NPC1L1 deficiency on cholesterol metabolism in mice on an HFD containing no added cholesterol. To fill this gap in knowledge, we examined cholesterol balance in LI-KO mice on an HFD. Consistent with a critical role of NPC1L1 in intestinal cholesterol absorption, LI-KO versus WT mice displayed a 97% reduction in intestinal cholesterol absorption

(Fig. 1A) and a 91% increase in fecal excretion rate of neutral sterols (cholesterol and its bacterial metabolites) (Fig. 1B). Because our HFD contains almost no cholesterol, these increased fecal neutral sterols must come from biliary and perhaps intestinal (37, 38) secretion of endogenously synthesized cholesterol. To compensate for excessive loss of cholesterol from the body, hepatic endogenous cholesterol synthesis was increased by  $\sim 7$ -fold (Fig. 1C) and transcripts of cholesterol biosynthetic enzymes, such as 3-hydroxy-3-methyl-glutaryl CoA (HMG-CoA) reductase, HMG-CoA synthase, and squalene synthase, were all up-regulated in L1-KO livers (supplementary Table 1). Despite this compensatory mechanism, plasma levels of total cholesterol, free cholesterol, cholesteryl ester, and hepatic contents of total cholesterol and cholesteryl ester were significantly reduced in L1-KO relative to WT mice on an HFD for 24 weeks (Fig. 1D, E), and their levels were similar to those observed in chow-fed animals.

### NPC1L1 deficiency prevents HFD-induced hepatic steatosis

To determine if genetic ablation of NPC1L1 influences HFD-induced hepatic steatosis, we examined livers from mice on an HFD for 24 weeks. As expected, livers from WT mice were enlarged (Table 1) and appeared grossly pale (not shown). H and E staining of sections from these livers revealed that hepatocytes were filled with multilobular droplets of varying sizes (Fig. 2A). Strikingly, these HFD-induced pathological abnormalities were completely absent in livers from L1-KO mice. The liver histology of HFD-fed L1-KO mice was similar to that of chow-fed WT mice (Fig. 2A). In addition, H and E staining revealed no signs of inflammatory leukocyte infiltration in livers of L1-KO mice fed an HFD and WT mice on both diets. The hepatic triglyceride content was 93% lower in L1-KO than WT mice on an HFD (Fig. 2B). Compared with chow-fed WT mice, the hepatic triglyceride content was increased by  $\sim 14$ -fold in HFD-fed WT mice (Fig. 2B).

### NPC1L1 deficiency prevents HFD-induced insulin resistance

Although an HFD may promote fat accumulation in the liver by simply providing more substrates for triglyceride synthesis, an important mechanism whereby an HFD may drive hepatic steatosis is by causing selective insulin resistance (26). The increased circulating insulin fails to suppress hepatic gluconeogenesis but can promote hepatic lipogenesis (25). To establish the relationship between hepatic steatosis and plasma insulin levels in our animal models, plasma insulin and glucose concentrations were measured under different diet conditions. As expected, 12 weeks of HFD feeding in WT mice significantly increased the plasma insulin level under both fed and fasted states and this increase was completely blunted in L1-KO mice (Fig. 3A). After 24 weeks on an HFD, the plasma insulin level was  $\sim 85\%$  lower in L1-KO than WT mice after a 4 h fast. Despite reduced plasma insulin levels, L1-KO mice, when compared with WT mice, were able to maintain similar plasma glucose in fed and 4 h-fasted states and even had significantly lower plasma glucose concentrations after overnight fasting (Fig. 3A), suggesting an insulin sensitive state. Indeed, when the glucose  $\times$  insulin index, an indicator of insulin sensitivity (39), was calculated by multiplying plasma insulin and corresponding glucose concentrations, the index was 67% and 81% lower in L1-KO than WT mice under fed and fasted states, respectively, similar to those in the chow-fed mice (Fig. 3A). To determine the glucose tolerance and systemic insulin sensitivity, we performed glucose and insulin tolerance tests. As expected, 16 weeks of HFD feeding in WT mice impaired glucose tolerance and reduced insulin sensitivity (Fig. 3B, C). Surprisingly, HFD-induced glucose intolerance was not improved in L1-KO mice (Fig. 3B). However, the systemic insulin sensitivity was increased in HFD-fed L1-KO mice relative to HFD-fed WT mice (Fig. 3C). The glucose intolerance seen in HFD-fed L1-KO mice may be attributable to reduced plasma insulin levels (Fig. 3A). To examine

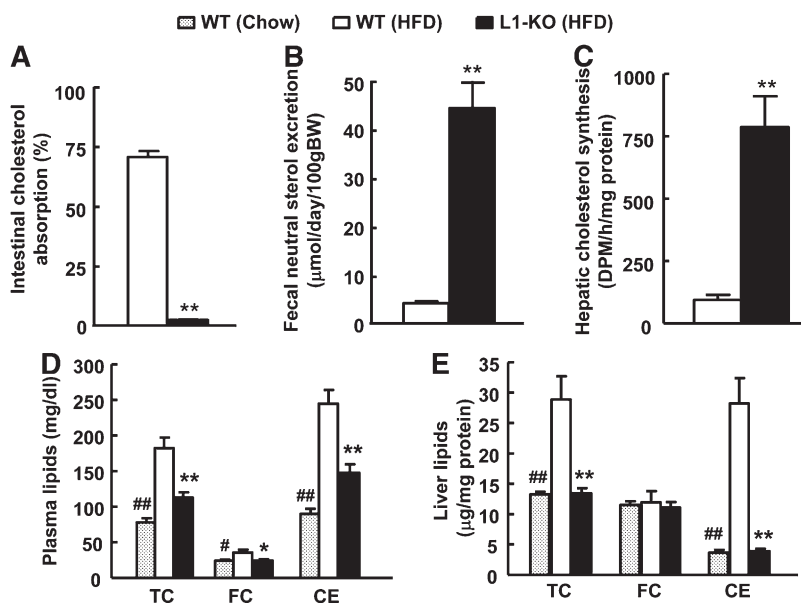


**Fig. 1.** L1-KO mice on an HFD have (A) reduced intestinal cholesterol absorption, (B) increased fecal neutral sterol excretion, (C) elevated endogenous hepatic cholesterol synthesis, and decreased plasma (D) and hepatic (E) cholesterol. The amount of cholesteryl ester (CE) was calculated by subtracting free cholesterol (FC) from total cholesterol (TC) and multiplying by 1.67 to convert to cholesteryl ester mass. \* $P < 0.05$ , \*\* $P < 0.001$ , L1-KO relative to wild-type (WT) mice on a high-fat diet (HFD); # $P < 0.05$ , ## $P < 0.001$ , WT mice on chow diet compared with WT mice on an HFD ( $n = 5-7$ ).

TABLE 1. L1-KO mice are resistant to HFD-induced obesity

	WT (Chow)	WT (HFD)	L1-KO (HFD)
BW (g)	30.0 ± 1.6 <sup>#</sup>	41.1 ± 2.3	26.5 ± 0.7**
WAT weight (g)	0.99 ± 0.24 <sup>#</sup>	3.05 ± 0.32	0.90 ± 0.07**
WAT/BW ratio	0.02 ± 0.008 <sup>##</sup>	0.07 ± 0.005	0.03 ± 0.002**
Liver weight (g)	1.15 ± 0.05 <sup>##</sup>	2.32 ± 0.26	0.99 ± 0.05*
Liver/BW ratio	0.04 ± 0.001 <sup>##</sup>	0.06 ± 0.004	0.04 ± 0.001*
Food Intake (g/day)	N.D.	2.2 ± 0.1	2.3 ± 0.1
Plasma triglyceride (mg/dl)	71.2 ± 7.28 <sup>#</sup>	36.7 ± 6.53	26.8 ± 5.45
Plasma NEFA (mmol/L)	N.D.	0.89 ± 0.06	0.73 ± 0.06
Plasma adiponectin (µg/ml)	N.D.	7.03 ± 0.42	5.88 ± 0.41
Plasma β-hydroxybutyrate (mmol/L)	N.D.	0.32 ± 0.04	0.39 ± 0.07

Food intake was measured in mice on an HFD for 20 weeks. Body weight (BW), tissue and plasma parameters were determined in mice on chow or an HFD for 24 weeks. Each value represents the mean ± SEM of 6–8 values. \* $P < 0.05$ , \*\* $P < 0.001$  (L1-KO relative to WT mice on HFD); <sup>#</sup> $P < 0.05$ , <sup>##</sup> $P < 0.001$  (WT mice on chow relative to WT mice on an HFD). WAT, white adipose tissue; NEFA, nonesterified fatty acid; N.D., not determined.

this possibility, plasma insulin levels were measured during glucose tolerance tests. Consistently, HFD-fed L1-KO mice had similar plasma insulin concentrations to the chow-fed mice, which were significantly lower than those in the HFD-fed WT mice before and after glucose challenge despite the cumulative increase in plasma insulin levels being similar between genotypes and between diet groups (Fig. 3D). The fact that the significantly lower plasma insulin level in HFD-fed L1-KO mice was able to maintain the plasma glucose concentration to the level seen in the hyperinsulinemic HFD-fed WT mice further supports that L1-KO mice were more insulin sensitive.

#### NPC1L1 deficiency prevents HFD-induced obesity

Because reduced hepatic steatosis itself may contribute to improved insulin sensitivity (26), the cause-effect relationship between hepatic steatosis and insulin resistance in L1-KO mice remains to be established. Interestingly, L1-KO mice were recently shown to resist HFD-induced obesity (16). Improved insulin sensitivity seen in L1-KO

mice may result partly from a reduction in HFD-induced weight gain. In this long-term HFD study, we monitored weight gain and food intake in our mice. Compared with a chow diet, HFD feeding dramatically promoted body weight gain and a 2-fold increase in epididymal fat pad weight in WT mice (Table 1). Although L1-KO and WT mice gained weight continuously during the diet period, after 24 weeks on an HFD, L1-KO mice weighed ~35.5% less than WT mice, which was associated with a 70% reduction in epididymal fat pad weight (Table 1). No differences were observed for plasma triglyceride, nonesterified fatty acids, adiponectin, and the ketone body β-hydroxybutyrate between L1-KO and WT mice on an HFD (Table 1).

The reduced weight gain in L1-KO mice could not be explained by a reduction in food intake because both L1-KO and WT mice consumed the same amount of food daily (Table 1). A previous study showed that L1-KO mice on an HFD have a moderate but significant reduction in intestinal fat absorption as assessed by a very sensitive and accurate method (16). Using the same method (29), we found that the intestinal total fatty acid absorption was reduced by 7.8% (Fig. 4A) with greater reductions observed for fatty acids C18:0 and 16:0 that were decreased by 12.9% and 8.7% (Fig. 4B), respectively, in L1-KO versus WT mice.

#### Hepatic de novo fatty acid synthesis is significantly reduced in L1-KO relative to WT mice on an HFD

To gain more insight into the protective mechanisms of NPC1L1 deficiency on hepatic steatosis in L1-KO mice, we examined hepatic levels of mRNAs for genes involved in lipogenesis, fatty acid oxidation, glucose metabolism, and LXR activation by qPCR. As seen in supplementary Table II, hepatic mRNA levels of all the lipogenic genes examined were lower in L1-KO than WT mice including malic enzyme, acetyl CoA carboxylase 1, fatty acid synthase, stearoyl CoA desaturase-1, and glycerol 3-phosphate acyltransferase 1. Glucokinase is an enzyme that activates glucose to form glucose-6-phosphate, a common substrate for both fatty acid synthesis and glycolysis, thus playing a

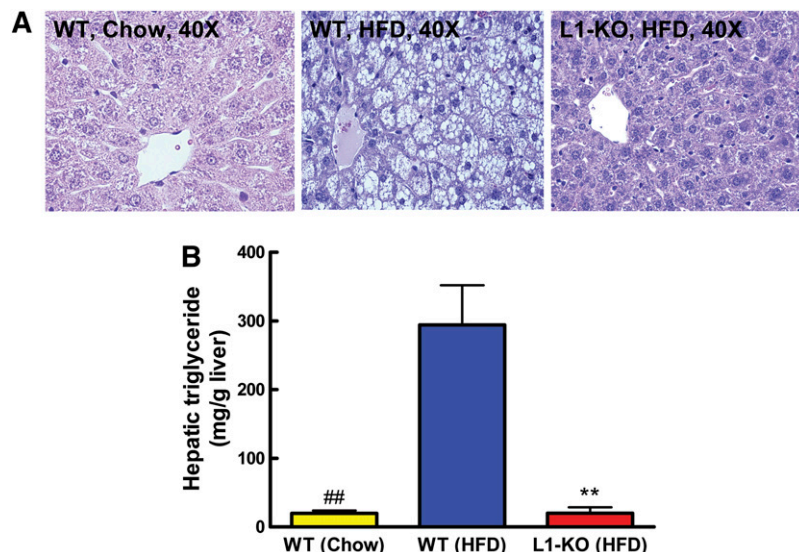
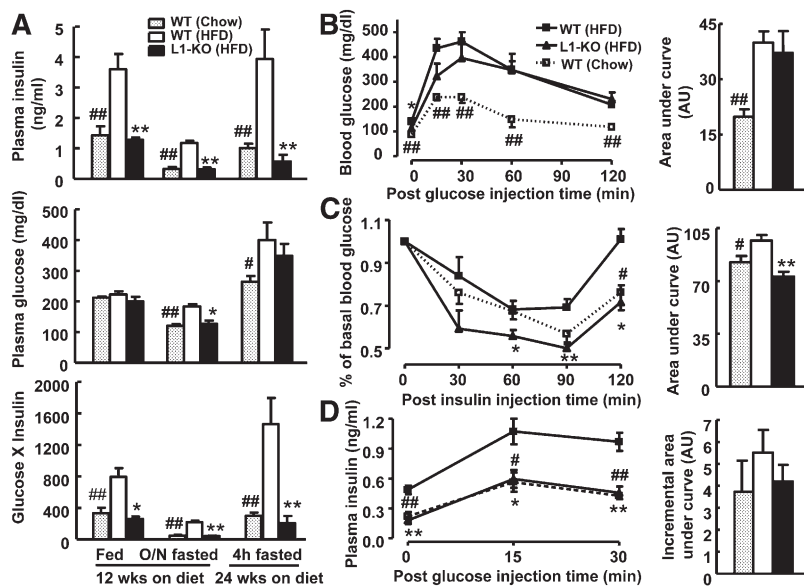


Fig. 2. L1-KO mice are resistant to HFD-induced hepatic steatosis. Livers were collected from WT male mice on both chow and an HFD and L1-KO male mice fed an HFD for 24 weeks. A: Representative H and E staining of liver sections. B: Hepatic triglyceride content (n = 6–7), \*\* $P < 0.001$ , L1-KO relative to WT mice on an HFD; <sup>##</sup> $P < 0.001$ , WT mice on chow diet compared with WT mice on an HFD.



**Fig. 3.** L1-KO relative to WT mice on an HFD are more insulin sensitive. A: Plasma levels of insulin and glucose, and the index of insulin sensitivity (insulin x glucose) in fed and overnight (O/N) fasted mice on an HFD or chow diet for 12 weeks and in 4 h fasted (during daylight cycle) mice on an HFD or chow diet for 24 weeks (n = 5–6). B: Glucose tolerance test in mice fed an HFD or chow diet for 16 weeks (n = 5–7). C: Insulin tolerance test in mice fed an HFD or chow diet for 15 weeks (n = 5). D: Glucose-stimulated insulin secretion in mice fed an HFD or chow diet for 5 weeks (n = 5–6). The area under the curve for glucose tolerance test and insulin tolerance test, and the incremental area under the curve for glucose-stimulated insulin secretion were calculated and shown in the right panel of each respective figure. AU, arbitrary unit. \**P* < 0.05, \*\**P* < 0.01, L1-KO versus WT mice on an HFD for the same treatment or at the same time point. #*P* < 0.05, ##*P* < 0.01, WT mice on chow versus an HFD for the same treatment or at the same time point.

critical role in hepatic lipogenesis and blood glucose homeostasis. Intriguingly, the hepatic mRNA level for this rate-limiting enzyme in converting glucose to fat was substantially reduced in L1-KO versus WT livers, which may reflect its positive regulation by insulin (40, 41). Because we measured mRNA levels by using pooled samples, we measured hepatic levels of mRNAs for SREBP-1c, acetyl CoA carboxylase 1, and glucokinase in individual samples in each group. They were significantly reduced (Fig. 5A), in line with data from pooled samples. Furthermore, we measured de novo hepatic fatty acid synthesis and it was significantly decreased by 63% in L1-KO compared with WT mice on an HFD (Fig. 5B).

Carbohydrate responsive element-binding protein (ChREBP) is a glucose sensor (42). Hepatic levels of mRNAs for this gene and genes in gluconeogenesis such as phosphoenolpyruvate carboxykinase and glucose-6-phosphatase were similar between L1-KO and WT mice (supplementary Table II).

To determine if NPC1L1 deficiency reduced hepatic steatosis by increasing fatty acid oxidation, we examined hepatic levels of mRNAs for peroxisome proliferator-activated receptor  $\alpha$ , peroxisome proliferator-activated receptor  $\gamma$  coactivator-1 $\alpha$  and peroxisome proliferator-activated receptor  $\gamma$  coactivator-1 $\beta$ , acyl-CoA oxidase, and carnitine palmitoyltransferase-1 (supplementary Table II). Although hepatic mRNA levels of acyl-CoA oxidase and carnitine palmitoyltransferase-1 were lower in L1-KO mice relative to WT mice, hepatic fatty acid oxidation activity was similar between the two genotypes (Fig. 5C).

To examine if NPC1L1 deficiency reduces hepatic steatosis by increasing lipoprotein triglyceride secretion, we measured plasma triglyceride concentrations at various time points after blocking triglyceride hydrolysis with Tyloxapol. Under this condition, L1-KO and WT mice had similar plasma triglyceride concentrations (Fig. 5D). The hepatic triglyceride secretion rates were calculated and were virtually identical between the two genotypes (Fig. 5E).

Increased hepatic triglyceride hydrolysis may attenuate fat accumulation in liver. To examine this possibility, we measured the hepatic triglyceride hydrolase activity in L1-KO and WT mice fed an HFD for 24 weeks and no differences were found (Fig. 5F).

#### NPC1L1 deficiency reduces hepatic oxidative stress

Protection against lipid accumulation may prevent lipid peroxidation in liver. To examine this possibility, we measured hepatic malondialdehyde, a product of lipid peroxidation, as TBARS. After 24 weeks of HFD feeding, the hepatic content of malondialdehyde was significantly reduced by ~29% in L1-KO versus WT mice (Fig. 6A). To assess the oxidative state of livers, we measured hepatic GSH/GSSG ratio in our mice. The GSH/GSSG ratio was slightly but significantly increased in L1-KO livers relative to WT livers (Fig. 6B).

#### DISCUSSION

This study was the first to systemically and mechanistically examine how genetic inactivation of NPC1L1 in mice prevents HFD-induced fatty liver. In this study, we not only

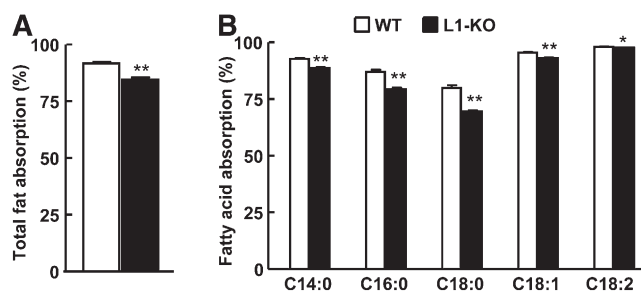


**Fig. 4.** L1-KO mice on an HFD have reduced intestinal absorption of total fatty acids (A) and specific fatty acid species (B). \**P* < 0.05; \*\**P* < 0.001 (n = 6).

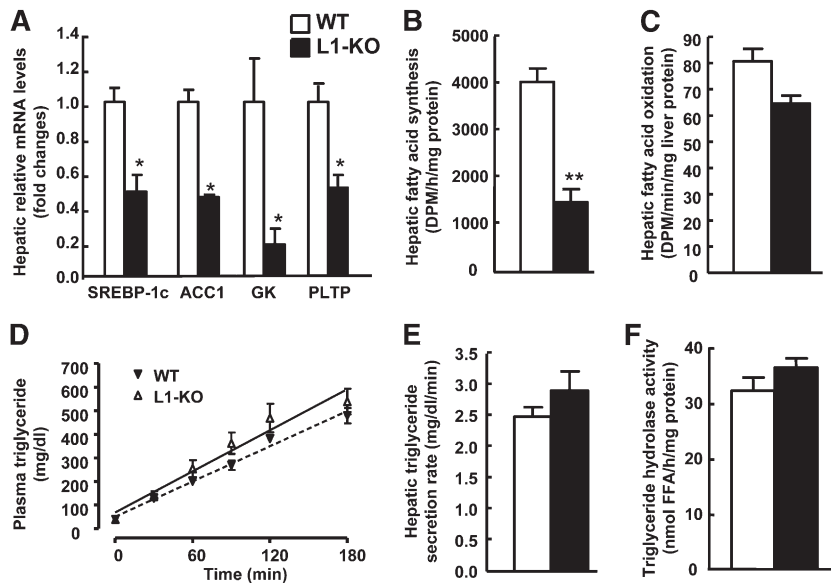


**Fig. 5.** L1-KO relative to WT mice show reduced hepatic fatty acid synthesis. A: Hepatic mRNA levels of genes involved in endogenous lipogenesis and an LXR target phospholipid transport protein (PLTP). Hepatic mRNA levels were measured by qPCR with individual total RNA samples from each group (n = 3). Cyclophilin was used as an internal control. Hepatic fatty acid synthesis (B) and fatty acid oxidation (C) in 4 h fasted mice on an HFD for 6 weeks (n = 6). D: Plasma triglyceride levels before and after Tyloxapol injection. E: Hepatic triglyceride secretion rates in mice on an HFD for 4 weeks (n = 5). F: Hepatic triglyceride hydrolase activity in mice on an HFD for 24 weeks (n = 6). \* $P < 0.05$ ; \*\* $P < 0.001$ . ACC1, acetyl CoA carboxylase 1; GK, glucokinase.

showed that NPC1L1 deficiency prevents HFD-induced hepatic steatosis, weight gain, and insulin resistance, but also demonstrated that these phenotypic alterations are associated with reduced circulating insulin levels, hepatic de novo fatty acid synthesis, and hepatic levels of mRNAs for lipogenic genes including glucokinase, an enzyme critical in conversion of glucose to fat. Given that elevated blood insulin increases hepatic lipogenic gene expression via transcription factors such as SREBP-1c (23, 42), and glucokinase is an important mediator in this lipogenic pathway (43), our data demonstrated for the first time that NPC1L1 deficiency in mice protects against HFD-induced hepatic steatosis by reducing hepatic lipogenesis at least in part through preventing HFD-induced insulin resistance and the associated hyperinsulinemia. Our findings, together with early reports showing that ezetimibe improves hepatic steatosis in rodents (12–15) and rabbits (44), warrant further studies of ezetimibe and NPC1L1 effects on fatty liver diseases and associated metabolic disorders.

Increased insulin sensitivity in L1-KO mice was supported by significantly lower plasma insulin levels in both fed and fasted states (Fig. 3A), systemic insulin sensitivity measured by insulin tolerance test (Fig. 3C), and lower insulin levels during the glucose stimulation (Fig. 3D). During the glucose tolerance test, L1-KO mice were glucose intolerant (Fig. 3B), which may be related to the substantially lower plasma insulin levels in these animals. The lower index of insulin sensitivity (glucose  $\times$  insulin) (Fig. 3A) further supports improved insulin sensitivity in L1-KO mice because it indicates that these animals require less insulin to maintain the plasma glucose to the level seen in WT mice whose

plasma insulin is much higher compared with L1-KO mice. It is currently unclear how NPC1L1 deficiency prevents HFD-induced insulin resistance and hyperinsulinemia. The major defect in L1-KO mice is the blockade of intestinal cholesterol absorption, which results in cholesterol deficit in the body. Interestingly, depletion of cell membrane cholesterol content has been shown to improve insulin sensitivity in cultured adipocytes (45, 46). Statins, which lower blood cholesterol by inhibiting HMG-CoA reductase activity, have been reported to improve insulin sensitivity in human subjects with metabolic syndrome (47, 48). It is possible that NPC1L1 deficiency prevents HFD-induced insulin resistance by reducing whole-body cholesterol pool. Alternatively, the reduced weight gain may partly explain the insulin sensitive phenotype in L1-KO mice.

It has yet to be molecularly elucidated how genetic inactivation of NPC1L1 in mice prevents HFD-induced obesity.

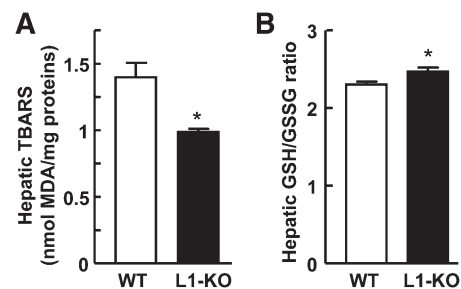


**Fig. 6.** L1-KO mice display reduced hepatic oxidative stress. A: Hepatic content of malondialdehyde (MDA) as TBARS (n = 6). B: Hepatic GSH/GSSG ratio (n = 4). \* $P < 0.05$ .

The daily food intake was similar between WT and L1-KO mice (Table 1) and the total intestinal fat absorption was reduced only by 7.8% in L1-KO mice (Fig. 4A), suggesting that the reduced energy intake is an unlikely explanation and L1-KO mice may have increased energy expenditure or thermogenesis. Intriguingly, we found that increasing the amount of cholesterol in an HFD to a level similar to that in a typical Western diet suffices to rescue HFD-induced weight gain in L1-KO mice (49), indicating the involvement of cholesterol-dependent mechanisms. Dietary cholesterol has been implicated in the regulating of diet-induced obesity in LXR deficient mice through unknown mechanisms (50), though the effect appears to be opposite to what we have seen in L1-KO mice. Nevertheless, further studies are warranted to molecularly define how dietary cholesterol regulates fat storage.

In the absence of dietary cholesterol such as in our HFD, NPC1L1 mainly mediates reabsorption of bile-derived cholesterol, thereby preventing excessive loss of endogenous cholesterol. L1-KO relative to WT mice on an HFD have reduced hepatic and plasma cholesterol due to reduced intestinal reabsorption and increased fecal excretion of endogenously derived cholesterol (Fig. 1). Excessive amounts of cholesterol are lipogenic through activation of LXR by its metabolites (20, 51). In this study, the hepatic levels of mRNAs for two LXR target genes, ATP-binding cassette transporter G5 and phospholipid transfer protein, were lower in L1-KO than WT mice. In a previous study, we also showed that T0901317, a synthetic LXR agonist, does not significantly increase hepatic triglyceride in L1-KO mice as it does in WT mice (22). Thus, NPC1L1 deficiency may have prevented HFD-induced hepatic steatosis in part by reducing cholesterol-dependent LXR activation in liver (Fig. 7).

Intestinal fat absorption was reduced by 7.8% in L1-KO mice (Fig. 4A). Although this small reduction in fat absorption cannot explain the more than 90% reduction in hepatic triglyceride, it may account for a small proportion of the decrease in overnutrition-induced hepatic steatosis over long periods. An important question is, how does a cholesterol transporter modulate fat absorption? A potential mechanism may be that inhibition of intestinal cholesterol absorption somehow alters intestinal expression of genes involved in fatty acid uptake and transport. Consistent with this, fatty acid transport protein (FATP) 4 was reported to be reduced in the small intestine of L1-KO mice on an HFD (16). We also found that mRNAs for FATP4 and another fatty acid transporter Cluster Determinant (CD) 36 were substantially reduced in the jejunum of L1-KO versus WT mice (supplementary Table I).

Elevated plasma glucose not only stimulates insulin secretion from pancreatic  $\beta$ -cells, but also activates ChREBP, a transcription factor that promotes hepatic glycolysis and lipogenesis (42). In this study, blood glucose levels were comparable between L1-KO and WT mice in the fed state and during glucose challenge (Fig. 3A, B). However, in the overnight-fasted L1-KO mice, plasma glucose is lower (Fig. 3A) and additionally, the reduction in glucokinase mRNA suggests that conversion of glucose to fat may be

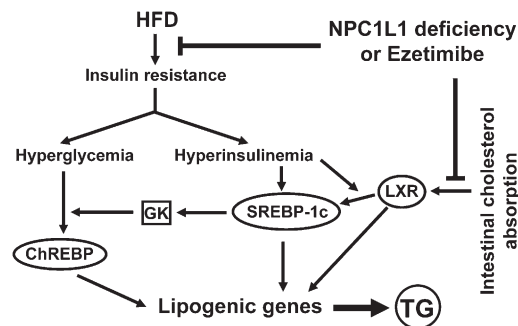


**Fig. 7.** Outline of known pathways involved in hepatic steatosis induced by an HFD and cholesterol, and potential roles of NPC1L1 deficiency or ezetimibe treatment in modulating these pathways. An HFD causes insulin resistance, a state that is associated with hyperinsulinemia and hyperglycemia. Elevated blood insulin and glucose activate transcription factors SREBP-1c and ChREBP, respectively, to increase hepatic lipogenic gene expression. Glucokinase (GK) plays a critical role in these lipogenic pathways. Intestinal cholesterol absorption promotes hepatic lipogenesis via cholesterol-dependent activation of LXR. NPC1L1 deficiency or ezetimibe treatment can block: 1) HFD-induced insulin resistance in part by reducing intestinal fat absorption and weight gain, and 2) cholesterol-driven lipogenesis by inhibiting intestinal cholesterol absorption, which together may substantially suppress hepatic triglyceride (TG) synthesis, thereby preventing dietary fat-induced hepatic steatosis.

decreased, which may also partly contribute to the steatoprotective role of NPC1L1 deficiency.


Another factor known to promote hepatic steatosis is the increased flux of free fatty acids into the liver as a result of increased fat lipolysis. Donnelly et al. (52) reported that in subjects with NAFLD, the plasma free fatty acid pool accounted for ~60% of triglyceride content in liver. Under normal physiological states, free fatty acids are stored in adipose tissue as triglyceride but in the insulin resistant adipose tissue, insulin fails to fully suppress fat lipolysis, resulting in increased release of free fatty acids into blood. However, the plasma concentrations of nonesterified fatty acids were similar between L1-KO and WT mice on an HFD (Table 1), arguing against an important role of fat lipolysis in modulating hepatic steatosis in our model.

Increases in fatty acid oxidation, triglyceride hydrolysis, and triglyceride secretion via lipoproteins in liver may prevent hepatic steatosis but we found that the hepatic fatty acid oxidation activity, triglyceride hydrolase activity, and triglyceride secretion rates are similar between L1-KO and WT mice (Fig. 5). In addition, plasma concentrations of  $\beta$ -hydroxybutyrate and triglyceride are comparable between the two genotypes (Table 1). Collectively, these findings demonstrate that the aforementioned factors were unlikely to have played an important role in protecting L1-KO mice from hepatic steatosis.

It was recently reported that leptin receptor deficient Zucker rats treated with ezetimibe have reduced hepatic reactive oxygen species (ROS), endoplasmic reticulum (ER) stress, and mitochondrial cholesterol, and based on these observations, the authors hypothesized that liver NPC1L1 contributes to hepatic insulin resistance through



free cholesterol accumulation and subsequent ROS generation and ER stress (13). Although this hypothesis is attractive and we also observed a reduction in hepatic oxidative stress in LI-KO relative to WT mice (Fig. 6), two important points should be made: 1) NPC1L1 protein is undetectable in rodent livers and the effect could be a result of NPC1L1 inhibition by ezetimibe in intestine rather than liver; and 2) although ROS generation and ER stress can cause hepatic steatosis, hepatic steatosis can also cause these cellular disorders, making it difficult to establish a cause-effect relationship.

Figure 7 summarizes the potential roles of NPC1L1 deficiency or ezetimibe treatment in protecting liver from steatosis induced by an HFD and cholesterol. Our data suggest that genetic deletion of NPC1L1 in mice may protect against HFD-induced hepatic steatosis mainly by preventing HFD-induced insulin resistance and hyperinsulinemia. Suppression of other lipogenic factors such as cholesterol-dependent LXR activation and glucose-dependent ChREBP activation may have contributed in part to the beneficial effects of NPC1L1 deficiency on fatty liver development. Further studies are required to define how NPC1L1, a cholesterol transporter that mainly mediates intestinal cholesterol absorption in rodents, modulates HFD-induced insulin resistance and obesity. 

The authors thank Drs. Yiannis A. Ioannou and Joanna P. Davies in the Department of Human Genetics, Mount Sinai School of Medicine, New York, NY for providing NPC1L1 knockout mice.

## REFERENCES

- Davies, J. P., B. Levy, and Y. A. Ioannou. 2000. Evidence for a Niemann-pick C (NPC) gene family: identification and characterization of NPC1L1. *Genomics*. **65**: 137–145.
- Altmann, S. W., H. R. Davis, Jr., L. J. Zhu, X. Yao, L. M. Hoos, G. Tetzloff, S. P. Iyer, M. Maguire, A. Golovko, M. Zeng, et al. 2004. Niemann-Pick C1 Like 1 protein is critical for intestinal cholesterol absorption. *Science*. **303**: 1201–1204.
- Davies, J. P., C. Scott, K. Oishi, A. Liapis, and Y. A. Ioannou. 2005. Inactivation of NPC1L1 causes multiple lipid transport defects and protects against diet-induced hypercholesterolemia. *J. Biol. Chem.* **280**: 12710–12720.
- Temel, R. E., W. Tang, Y. Ma, L. L. Rudel, M. C. Willingham, Y. A. Ioannou, J. P. Davies, L. M. Nilsson, and L. Yu. 2007. Hepatic Niemann-Pick C1-like 1 regulates biliary cholesterol concentration and is a target of ezetimibe. *J. Clin. Invest.* **117**: 1968–1978.
- Davis, H. R., Jr., L. J. Zhu, L. M. Hoos, G. Tetzloff, M. Maguire, J. Liu, X. Yao, S. P. Iyer, M. H. Lam, E. G. Lund, et al. 2004. Niemann-Pick C1 Like 1 (NPC1L1) is the intestinal phytosterol and cholesterol transporter and a key modulator of whole-body cholesterol homeostasis. *J. Biol. Chem.* **279**: 33586–33592.
- Davis, H. R., Jr., L. M. Hoos, G. Tetzloff, M. Maguire, L. J. Zhu, M. P. Graziano, and S. W. Altmann. 2007. Deficiency of Niemann-Pick C1 Like 1 prevents atherosclerosis in ApoE<sup>-/-</sup> mice. *Arterioscler. Thromb. Vasc. Biol.* **27**: 841–849.
- Garcia-Calvo, M., J. Lisnock, H. G. Bull, B. E. Hawes, D. A. Burnett, M. P. Braun, J. H. Crona, H. R. Davis, Jr., D. C. Dean, P. A. Detmers, et al. 2005. The target of ezetimibe is Niemann-Pick C1-Like 1 (NPC1L1). *Proc. Natl. Acad. Sci. USA*. **102**: 8132–8137.
- Weinglass, A. B., M. Kohler, U. Schulte, J. Liu, E. O. Nketiah, A. Thomas, W. Schmalhofer, B. Williams, W. Bildl, D. R. McMasters, et al. 2008. Extracellular loop C of NPC1L1 is important for binding to ezetimibe. *Proc. Natl. Acad. Sci. USA*. **105**: 11140–11145.
- Davis, H. R., and E. P. Veltri. 2007. Zetia: inhibition of Niemann-Pick C1 Like 1 (NPC1L1) to reduce intestinal cholesterol absorption and treat hyperlipidemia. *J. Atheroscler. Thromb.* **14**: 99–108.
- Chan, D. C., G. F. Watts, S. K. Gan, E. M. Ooi, and P. H. Barrett. 2010. Effect of ezetimibe on hepatic fat, inflammatory markers, and apolipoprotein B-100 kinetics in insulin-resistant obese subjects on a weight loss diet. *Diabetes Care*. **33**: 1134–1139.
- Yagi, S., M. Akaike, K. Aihara, T. Iwase, K. Ishikawa, S. Yoshida, Y. Sumitomo-Ueda, K. Kusunose, T. Niki, K. Yamaguchi, et al. 2010. Ezetimibe ameliorates metabolic disorders and microalbuminuria in patients with hypercholesterolemia. *J. Atheroscler. Thromb.* **17**: 173–180.
- Deushi, M., M. Nomura, A. Kawakami, M. Haraguchi, M. Ito, M. Okazaki, H. Ishii, and M. Yoshida. 2007. Ezetimibe improves liver steatosis and insulin resistance in obese rat model of metabolic syndrome. *FEBS Lett.* **581**: 5664–5670.
- Nomura, M., H. Ishii, A. Kawakami, and M. Yoshida. 2009. Inhibition of hepatic Nieman-Pick C1-Like 1 improves hepatic insulin resistance. *Am. J. Physiol. Endocrinol. Metab.* Epub ahead of print. August 4, 2009.
- Assy, N., M. Grozovski, I. Bersudsky, S. Szvalb, and O. Hussein. 2006. Effect of insulin-sensitizing agents in combination with ezetimibe, and valsartan in rats with non-alcoholic fatty liver disease. *World J. Gastroenterol.* **12**: 4369–4376.
- Zheng, S., L. Hoos, J. Cook, G. Tetzloff, H. Davis, Jr., M. van Heek, and J. J. Hwa. 2008. Ezetimibe improves high fat and cholesterol diet-induced non-alcoholic fatty liver disease in mice. *Eur. J. Pharmacol.* **584**: 118–124.
- Labonte, E. D., L. M. Camarota, J. C. Rojas, R. J. Jandacek, D. E. Gilham, J. P. Davies, Y. A. Ioannou, P. Tso, D. Y. Hui, and P. N. Howles. 2008. Reduced absorption of saturated fatty acids and resistance to diet-induced obesity and diabetes by ezetimibe-treated and Npc1l1<sup>-/-</sup> mice. *Am. J. Physiol. Gastrointest. Liver Physiol.* **295**: G776–G783.
- Browning, J. D., and J. D. Horton. 2004. Molecular mediators of hepatic steatosis and liver injury. *J. Clin. Invest.* **114**: 147–152.
- Clark, J. M. 2006. The epidemiology of nonalcoholic fatty liver disease in adults. *J. Clin. Gastroenterol.* **40**(Suppl 1): S5–S10.
- Browning, J. D., L. S. Szczepaniak, R. Dobbins, P. Nuremberg, J. D. Horton, J. C. Cohen, S. M. Grundy, and H. H. Hobbs. 2004. Prevalence of hepatic steatosis in an urban population in the United States: impact of ethnicity. *Hepatology*. **40**: 1387–1395.
- Janowski, B. A., P. J. Willy, T. R. Devi, J. R. Falck, and D. J. Mangelsdorf. 1996. An oxysterol signalling pathway mediated by the nuclear receptor LXR alpha. *Nature*. **383**: 728–731.
- Schultz, J. R., H. Tu, A. Luk, J. J. Repa, J. C. Medina, L. Li, S. Schwendner, S. Wang, M. Thoolen, D. J. Mangelsdorf, et al. 2000. Role of LXRs in control of lipogenesis. *Genes Dev.* **14**: 2831–2838.
- Tang, W., Y. Ma, L. Jia, Y. A. Ioannou, J. P. Davies, and L. Yu. 2008. Niemann-Pick C1-Like 1 is required for an LXR agonist to raise plasma HDL cholesterol in mice. *Arterioscler. Thromb. Vasc. Biol.* **28**: 448–454.
- Chen, G., G. Liang, J. Ou, J. L. Goldstein, and M. S. Brown. 2004. Central role for liver X receptor in insulin-mediated activation of Srebp-1c transcription and stimulation of fatty acid synthesis in liver. *Proc. Natl. Acad. Sci. USA*. **101**: 11245–11250.
- Horton, J. D., J. L. Goldstein, and M. S. Brown. 2002. SREBPs: activators of the complete program of cholesterol and fatty acid synthesis in the liver. *J. Clin. Invest.* **109**: 1125–1131.
- Brown, M. S., and J. L. Goldstein. 2008. Selective versus total insulin resistance: a pathogenic paradox. *Cell Metab.* **7**: 95–96.
- Shulman, G. I. 2000. Cellular mechanisms of insulin resistance. *J. Clin. Invest.* **106**: 171–176.
- Biddinger, S. B., K. Almind, M. Miyazaki, E. Kokkotou, J. M. Ntambi, and C. R. Kahn. 2005. Effects of diet and genetic background on sterol regulatory element-binding protein-1c, stearoyl-CoA desaturase 1, and the development of the metabolic syndrome. *Diabetes*. **54**: 1314–1323.
- Tang, W., Y. Ma, L. Jia, Y. A. Ioannou, J. P. Davies, and L. Yu. 2009. Genetic inactivation of NPC1L1 protects against sitosterolemia in mice lacking ABCG5/ABCG8. *J. Lipid Res.* **50**: 293–300.
- Jandacek, R. J., J. E. Heubi, and P. Tso. 2004. A novel, noninvasive method for the measurement of intestinal fat absorption. *Gastroenterology*. **127**: 139–144.
- Mulvihill, E. E., E. M. Allister, B. G. Sutherland, D. E. Telford, C. G. Sawyez, J. Y. Edwards, J. M. Markle, R. A. Hegele, and M. W. Huff. 2009. Naringenin prevents dyslipidemia, apolipoprotein B overproduction, and hyperinsulinemia in LDL receptor-null mice with diet-induced insulin resistance. *Diabetes*. **58**: 2198–2210.
- Linden, D., L. William-Olsson, A. Ahnmark, K. Ekroos, C. Hallberg, H. P. Sjogren, B. Becker, L. Svensson, J. C. Clapham, J. Oscarsson,

- et al. 2006. Liver-directed overexpression of mitochondrial glycerol-3-phosphate acyltransferase results in hepatic steatosis, increased triacylglycerol secretion and reduced fatty acid oxidation. *FASEB J.* **20**: 434–443.
32. Millar, J. S., D. A. Cromley, M. G. McCoy, D. J. Rader, and J. T. Billheimer. 2005. Determining hepatic triglyceride production in mice: comparison of poloxamer 407 with Triton WR-1339. *J. Lipid Res.* **46**: 2023–2028.
  33. Schweiger, M., G. Schoiswohl, A. Lass, F. P. Radner, G. Haemmerle, R. Malli, W. Graier, I. Cornaciu, M. Oberer, R. Salvayre, et al. 2008. The C-terminal region of human adipose triglyceride lipase affects enzyme activity and lipid droplet binding. *J. Biol. Chem.* **283**: 17211–17220.
  34. Radner, F. P., I. E. Streith, G. Schoiswohl, M. Schweiger, M. Kumari, T. O. Eichmann, G. Rechberger, H. C. Koefeler, S. Eder, S. Schauer, et al. 2010. Growth retardation, impaired triacylglycerol catabolism, hepatic steatosis, and lethal skin barrier defect in mice lacking comparative gene identification-58 (CGI-58). *J. Biol. Chem.* **285**: 7300–7311.
  35. Norris, A. W., L. Chen, S. J. Fisher, I. Szanto, M. Ristow, A. C. Jozsi, M. F. Hirshman, E. D. Rosen, L. J. Goodyear, F. J. Gonzalez, et al. 2003. Muscle-specific PPAR $\gamma$ -deficient mice develop increased adiposity and insulin resistance but respond to thiazolidinediones. *J. Clin. Invest.* **112**: 608–618.
  36. Yang, J., J. L. Goldstein, R. E. Hammer, Y. A. Moon, M. S. Brown, and J. D. Horton. 2001. Decreased lipid synthesis in livers of mice with disrupted Site-1 protease gene. *Proc. Natl. Acad. Sci. USA.* **98**: 13607–13612.
  37. Kruit, J. K., T. Plosch, R. Havinga, R. Boverhof, P. H. Groot, A. K. Groen, and F. Kuipers. 2005. Increased fecal neutral sterol loss upon liver X receptor activation is independent of biliary sterol secretion in mice. *Gastroenterology.* **128**: 147–156.
  38. van der Velde, A. E., C. L. Vriens, K. van den Oever, C. Kunne, R. P. Oude Elferink, F. Kuipers, and A. K. Groen. 2007. Direct intestinal cholesterol secretion contributes significantly to total fecal neutral sterol excretion in mice. *Gastroenterology.* **133**: 967–975.
  39. Xue, B., Y. B. Kim, A. Lee, E. Toschi, S. Bonner-Weir, C. R. Kahn, B. G. Neel, and B. B. Kahn. 2007. Protein-tyrosine phosphatase 1B deficiency reduces insulin resistance and the diabetic phenotype in mice with polygenic insulin resistance. *J. Biol. Chem.* **282**: 23829–23840.
  40. Iynedjian, P. B., A. Gjinovci, and A. E. Renold. 1988. Stimulation by insulin of glucokinase gene transcription in liver of diabetic rats. *J. Biol. Chem.* **263**: 740–744.
  41. Magnuson, M. A., T. L. Andreone, R. L. Printz, S. Koch, and D. K. Granner. 1989. Rat glucokinase gene: structure and regulation by insulin. *Proc. Natl. Acad. Sci. USA.* **86**: 4838–4842.
  42. Uyeda, K., and J. J. Repa. 2006. Carbohydrate response element binding protein, ChREBP, a transcription factor coupling hepatic glucose utilization and lipid synthesis. *Cell Metab.* **4**: 107–110.
  43. Dentin, R., J. P. Pegorier, F. Benhamed, F. Foufelle, P. Ferre, V. Fauveau, M. A. Magnuson, J. Girard, and C. Postic. 2004. Hepatic glucokinase is required for the synergistic action of ChREBP and SREBP-1c on glycolytic and lipogenic gene expression. *J. Biol. Chem.* **279**: 20314–20326.
  44. Ogawa, T., H. Fujii, K. Yoshizato, and N. Kawada. 2010. A human-type nonalcoholic steatohepatitis model with advanced fibrosis in rabbits. *Am. J. Pathol.* **177**: 153–165.
  45. Horvath, E. M., L. Tackett, and J. S. Elmendorf. 2008. A novel membrane-based anti-diabetic action of atorvastatin. *Biochem. Biophys. Res. Commun.* **372**: 639–643.
  46. Liu, P., B. J. Leffler, L. K. Weeks, G. Chen, C. M. Bouchard, A. B. Strawbridge, and J. S. Elmendorf. 2004. Sphingomyelinase activates GLUT4 translocation via a cholesterol-dependent mechanism. *Am. J. Physiol. Cell Physiol.* **286**: C317–C329.
  47. Guclu, F., B. Ozmen, Z. Hekimsoy, and C. Kirmaz. 2004. Effects of a statin group drug, pravastatin, on the insulin resistance in patients with metabolic syndrome. *Biomed. Pharmacother.* **58**: 614–618.
  48. Huptas, S., H. C. Geiss, C. Otto, and K. G. Parhofer. 2006. Effect of atorvastatin (10 mg/day) on glucose metabolism in patients with the metabolic syndrome. *Am. J. Cardiol.* **98**: 66–69.
  49. Jia, L., Y. Ma, G. Liu, and L. Yu. 2010. Dietary cholesterol reverses resistance to diet-induced weight gain in mice lacking Niemann-Pick C1-Like 1. *J. Lipid Res.* Epub ahead of print. July 2, 2010; doi: 10.1194/jlr.M008599.
  50. Kalaany, N. Y., K. C. Gauthier, A. M. Zavacki, P. P. Mammen, T. Kitazume, J. A. Peterson, J. D. Horton, D. J. Garry, A. C. Bianco, and D. J. Mangelsdorf. 2005. LXRs regulate the balance between fat storage and oxidation. *Cell Metab.* **1**: 231–244.
  51. Repa, J. J., G. Liang, J. Ou, Y. Bashmakov, J. M. Lobaccaro, I. Shimomura, B. Shan, M. S. Brown, J. L. Goldstein, and D. J. Mangelsdorf. 2000. Regulation of mouse sterol regulatory element-binding protein-1c gene (SREBP-1c) by oxysterol receptors, LXR $\alpha$  and LXR $\beta$ . *Genes Dev.* **14**: 2819–2830.
  52. Donnelly, K. L., C. I. Smith, S. J. Schwarzenberg, J. Jessurun, M. D. Boldt, and E. J. Parks. 2005. Sources of fatty acids stored in liver and secreted via lipoproteins in patients with nonalcoholic fatty liver disease. *J. Clin. Invest.* **115**: 1343–1351.